CONTRIBUTIONS to SCIENCE, **1** (3): 331-343 (2000)
Institut d'Estudis Catalans, Barcelona

Development and testing of galvanic anodes for cathodic protection

Joan Genescà*[1] and Julio Juárez[2]

1 Departamento de Ingeniería Metalúrgica. Facultad de Química. Universidad Nacional Autónoma de México (UNAM)

2 Instituto de Investigación en Materiales. Universidad Nacional Autónoma de México (UNAM)

Abstract

This paper summarizes the results obtained in the research project carried out in our laboratory related to the testing of sacrificial anodes used in cathodic protection (CP) systems and the development of new In/Hg-free aluminium-alloy anodes.

The main contributions are in the following subjects:

1. Corrosion mechanism during electrochemical testing.
   1.1. Al. Electrochemical testing of Al sacrificial anodes.
   1.2. Mg. Dissolution mechanism of Mg sacrificial anodes under electrochemical testing.
   1.3. Zn. EIS testing of thermal spray Zn anodes for concrete applications.
2. Improving the efficiency of Mg sacrificial anodes by microstructure control and heat treatments.
3. Design and development of new Al-alloy anodes In/Hg free.

The evaluation of an Al-Zn-Mg-Li alloy as a potential candidate for Al-sacrificial anode was studied.

The Al-Zn-Mg system was particularly selected due to the presence of precipitates in α-Al matrix which are capable of breaking down passive films whilst presenting good electrochemical efficiencies. The effect of Li additions on superficial activation of the anode by means of precipitation of AlLi type compounds was also examined.

Keywords: Aluminium, magnesium, zinc, sacrificial anodes, cathodic protection, electrochemical efficiency

Resum

Aquest treball resumeix els resultats obtinguts en un projecte de recerca dut a terme en el nostre laboratori i relacionat amb l'assaig electroquímic dels ànodes de sacrifici emprats en protecció catòdica, així com en el desenvolupament de nous ànodes d'alumini -Al- lliures d'indi -In- i de mercuri -Hg.

Les aportacions més importants han estat fetes en els aspectes següents:

1. Mecanisme de corrosió durant els assaigs electroquímics.
   1.1. Al. Assaig electroquímic d'ànodes de sacrifici de Al.
   1.2. Mg. Mecanisme de dissolució dels ànodes de sacrifici de Mg durant l'assaig electroquímic.
   1.3. Zn. L'impedància electroquímica com a eina d'assaig dels ànodes de sacrifici de Zn aplicats per projecció tèrmica sobre el formigó.
2. Augment de l'eficiència electroquímica dels ànodes de Mg mitjançant el tractament tèrmic i el control de la seva microestructura.
3. Disseny i desenvolupament de nous ànodes de Al sense In ni Hg.

Aquests nous ànodes de Al-Zn-Mg-Li són proposats com una alternativa als actualment en ús. El sistema Al-Mg-Zn ha estat escollit a causa de la presència de precipitats en la matriu de l'alumini, que poden ser capaços de trencar la pel·lícula passiva, però mantenen una alta eficiència electroquímica.

Background

One means of controlling corrosion is by the employment of cathodic protection. The first application of cathodic protection and statement of the principles of the technique were made by Sir Humphrey Davy in 1824. Using small buttons of zinc, or iron nails, attached to the protective copper sheathing installed on the hulls of wooden warships, Davy was able to arrest «the rapid decay of the copper» [1]. Cathodic protection can only by applied when the metal is exposed to an electrolytically conducting environment. Thus the application of the technique is virtually restricted to aqueous envi-

* Author for correspondence: Joan Genescà, Departamento de Ingeniería Metalúrgica, Facultad de Química, Universidad Nacional Autónoma de México (UNAM). México D.F., Mexico

ronments and the control of aqueous corrosion. This is not so great a restriction as may at first appear, since cathodic protection may be employed in moist soils and sands as well as in natural waters, brines and many aqueous process fluids.

Cathodic protection (CP) is surely the most often used method to prevent corrosion. The traditional use of cathodic protection has been to prevent corrosion of steel in the ground or water and this is still its most common application. It is now almost universally adopted on ships, oil rigs, and oil and gas pipelines. Over the last 50 years cathodic protection has advanced from being a black art to something approaching a science for these applications. Many excellent references are available which cover the theoretical and practical aspects of CP [2-8].

Corrosion is an electrochemical process of great economic importance estimated to consume 4% of the Gross National Product (GNP) of United States of America (USA) [9-11[JG1]]. This percentage is likely to be of the same order globally.

In all low-temperature corrosion reactions, for the reactions to occur an electrochemical cell is needed. This cell comprises an anode and cathode separated by an electrolyte with a metallic conduction. When a metal such as steel is used as an electrolyte, a corrosion cell can be formed. If steel is physically attached (i.e. welded, bolted or cast) to a piece of magnesium (Mg) and both are placed in an electrolyte, the Mg will form all the anode and the steel will only form the cathode. The resulting corrosion reactions will occur to the Mg which will be consumed. A balancing reduction reaction will occur to the steel, which will remain unaffected by its immersion in the electrolyte. This is the basis of cathodic protection (CP) [8]. When you cathodically protect steel or any other metal you alter its exclusive action as a cathode by the imposition of an external anode (sacrificial or galvanic anode), which will corrode preferentially.

One form of CP is termed «galvanic» (GCP) or «sacrificial» anode cathodic protection. With this system, electric current is applied by the employment of dissimilar metals, with the driving voltage being created by the potential generated between the steel and the anode in the electrolyte. The galvanic anodes are alloys of Mg, Zn and Al [1,8], which can be applied to protect steel in aqueous and soil environments.

1. Corrosion mechanism during electrochemical testing

Introduction

Testing of sacrificial anodes search for the following parameters [12]:

1. Closedcircuit electrochemical potential.
2. Longterm current output characteristics.
3. Current capacity per kilogram.
4. Corrosion characteristics.
5. Anode structure and soundness.

Electrochemical properties, potential, capacity and corrosion pattern are the most important references. The potential is a function of the alloy and the environment. The anode's electrochemical capacity represents a figure of the effectiveness of the anode alloys. Finally, a third important factor to be assessed is the corrosion pattern and nature of the corrosion products. An alloy that under testing produces a heavy and dense deposit is likely to be passivated, or to result in a rough-pitted surface during service. A good anode material supports a light, obviously porous deposit with a smooth clean surface underneath, which is likely to remain active throughout its service life. Of course, all the electrochemical properties also depend on the alloy's composition.

There are many ways of testing anodes for electrochemical properties. However, the testing should provide information for:

- production control,
- anode alloy control, and
- anode field-testing.

Among the test methods, galvanostatic testing is one of the most useful. Galvanostatic testing is common in corrosion research and is carried out by imposing a constant current on a test specimen and reading the resulting potential. In anode testing this method may also be used to determine the anode's current capacity. One special galvanostatic test is the hydrogen evolution test. Small impurities, which may not be detected by chemical analysis alone, can cause local cell action, which leads to lower anode efficiency. Hydrogen evolution is the primary cathodic reaction taking place at these local cells. Thus, its measurement affords an indirect determination of the loss of efficiency of the anode. NACE TM0190-98 is based in one of these tests [13].

The electrochemical behaviour of sacrificial anode materials is of vital importance for the reliability and efficiency of cathodic protection systems for seawaterexposed structures. From a practical point of view it is necessary to document service performance and quality level during current production throughout laboratory testing. For quality assurance (QA) purposes various methods are applied. These different electrochemical techniques giving either potentiostatic or galvanostatic control of test specimens or spontaneous galvanic coupling between the anode specimen and a defined cathode («free-running test»).

Cathodic protection design reliability depends to a large extent on input parameters used in design calculations. Some of the most important input parameters in these calculations are the electrochemical properties of sacrificial anodes. The electrochemical efficiency of the anode material is used for weight (lifetime) calculations and the anode potential (driving voltage) is used to calculate anode current output.

1.1 Aluminium Anodes. Electrochemical testing of Al sacrificial anodes

The testing of indium-activated, aluminium alloy sacrificial anode samples, using the procedures of Det Norske Veritas, DNV, RP B401, Appendix A, [14] is mainly intended to serve

as a QA/QC indicator regarding the electrochemical faradic efficiency and anode potential under cathodic protection conditions.

The recommended test procedure for quality control purposes [14, 15eurocorr99] is carried out galvanostatically with four subsequent current density levels each lasting 24 hours. Thus, total test duration is 96 hours.

In order to provide information about the behaviour of these anodes under DNV experimental conditions , samples were held galvanostatically at different current density levels, obtaining the impedance diagrams at the beginning and the end of each period [15].

Several aluminium-based alloys (generally Al-Zn-In type) have been tested [15,16]. Results show that the electrochemical performance of an Al sacrificial anode alloy is strongly dependent upon the formation of corrosion products on the surface. An anode in service will typically be covered with corrosion products and this influence on the electrochemical behaviour should be reflected in laboratory tests for performance documentation. The effect of chemical composition on electrochemical capacity has also been studied [15,16]. Higher Si, Cu and Fe content seem to be the main reason the capacity was lower than expected. The recommended maximum impurity levels given in RP B401 (Fe max. 0,1 wt.% and Si max 0,15wt%)[14] are within the range where no detrimental effects of these elements can be recorded.

Inhomogenities in the microstructure have been found to be of importance when indications of abnormal behaviour are indicated through short-term testing. Tendency to passivation can be attributed to a strong depletion of Zn in the matrix and a corresponding enrichment at the grain boundaries. This type of effect, which is probably related to quality control aspects of the production process, is very efficiently picked up in the short-term procedure test. Normally, inhomogenities and variations of anode alloy metallurgy and microstructure are reflected by a large scatter in the efficiencies recorded between the multiple specimens exposed. EIS has proved an interesting tool to reveal corrosion product formation on the surface of the anode, affecting electrochemical efficiency significantly. Nyquist diagrams such as the one shown in Figure 1, [15] is representative of this behaviour.

An active closed-circuit potential is desirable because a relatively noble potential could indicate the presence of passivation. Anodes must also possess high faradic efficiency in order to avoid frequent anode replacement. The NACE [13] and DNV [14] tests specifies that an Al anode should have a closed-circuit potential active to -1.0 V (SCE) and an electrochemical efficiency, ϵ, between 2300 and 2700 A-h/Kg [15]. Figure 3 indicates that corrosion products' resistance, R_{cp}, decreases, as current density increases . This is probably due to the fact that heavier and denser corrosion products form at higher current density, which will promote the self-corrosion activity. This would seem to prove the effect of corrosion product formation of on the self-corrosion rate of the anode. The self-corrosion rate will account for a relatively higher part of the total mass loss at lower anodic current densities. On partly consumed anodes where corrosion products have settled, the maintenance and development of the corrosion products will be more efficient at higher current densities than at lower. Consequently, the self-corrosion rate due to a more corrosive environment beneath the corrosion product will be correspondingly higher at high anodic current density.

It is evident from the electrochemical impedance data that the current density condition plays a critical role in the resistive property of the corrosion products, suggesting a significant change in the corrosion product property formed on the Al anode.

The lower electrochemical activity exhibited by the Al anode samples strongly suggests that local indium depletion may be the fundamental cause of this behaviour as previously proposed by Attanasio et al. [17]. The local In deple-

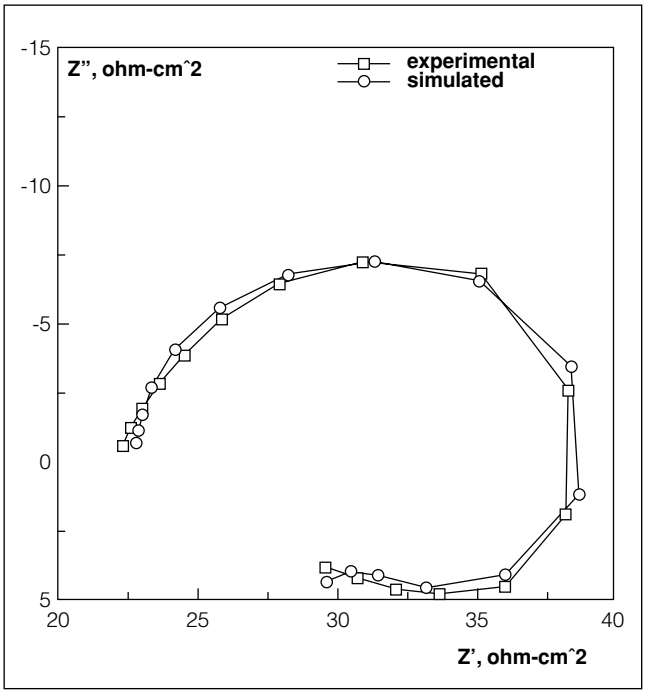

Figure 1. Nyquist plot for indium-activated aluminium alloy anode in ASTM seawater at 4 mA/cm^2.

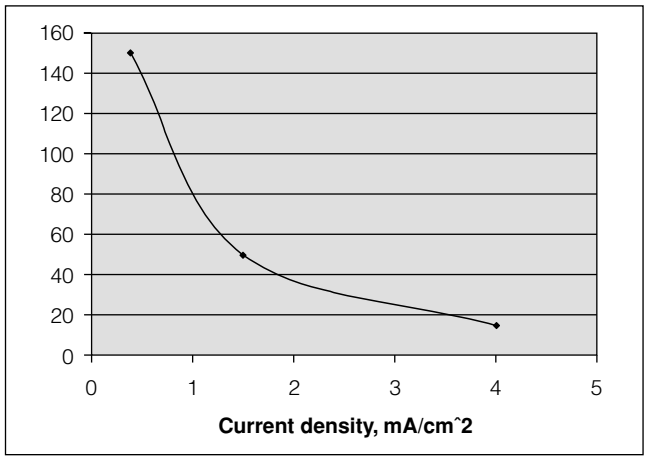

Figure 2. Electric resistance of corrosion products formed on Al anode in ASTM seawater at different current density values.

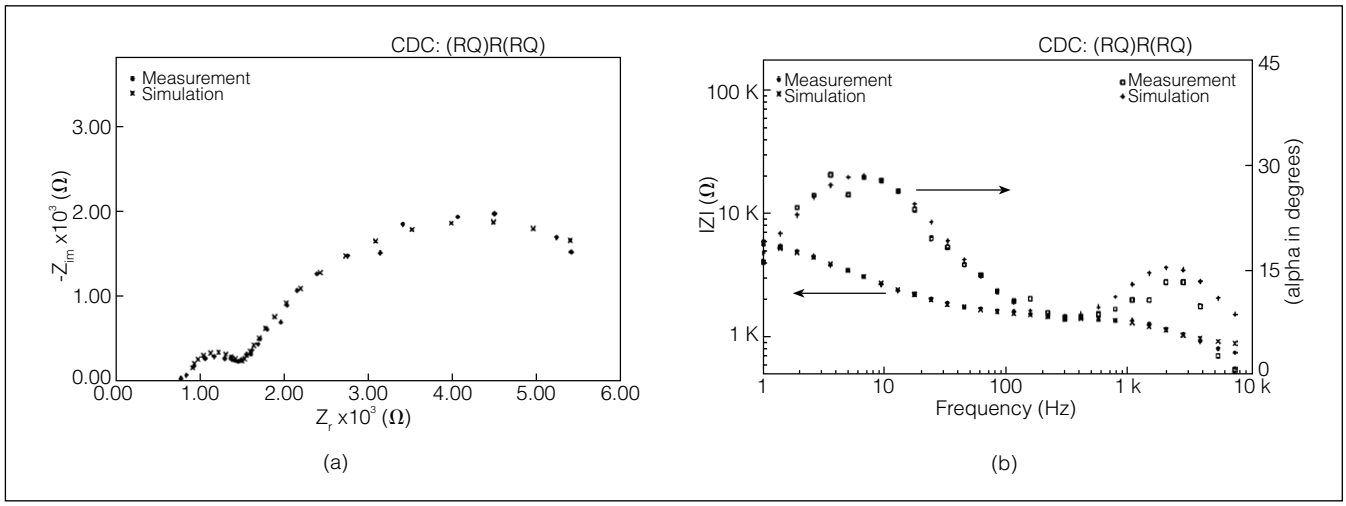

Figure 3. Typical impedance diagram: (a) Nyquist and (b) Bode representation of magnesium galvanic anode recorded during ASTM test [25].

tion could be the reason that Al anodes underwent pitting corrosion and did not achieve closed-circuit potentials more active than -0.950 V (SCE). In our experiments, the EIS diagrams obtained at higher current densities show an inductive semicircle [15], which could be attributed to pitting corrosion. The preferred dissolution morphology is general attack rather than pitting, since pitting attack has been correlated to less than optimal performance [18,19]. The existence of pitting attack is also consistent with the notion that In depletion is responsible for the observed behaviour, according to Uruchurtu [20] and Reboul et al. [21].

The anodic polarisation behaviour showed evidence of both passivation and pitting. The polarisation test is consistent with surface dissolution morphology, as the measured closed-circuit potential values were found to be located above the pitting or breakdown potential. The polarisation test was performed at the end of the short-term electrochemical test in order to determine anode behaviour type.

One argument in the past against using the short-term electrochemical test was that in the two-week [13] or four-day [14] test, only the outer 260 μm is consumed, whereas in the one-year test at least 0.5 cm penetration is realised. Murray et al. [22] have obtained successful results showing that by evaluating both the ascast material simultaneously with cut surfaces (which are representative of the bulk material) the short-term test appears to be quite representative of the cast anode long-term performance.

The primary areas of application for galvanic anodes to date have been in protection of exposed steel in aqueous environments, such as seawater, and for protection in damp, low resistivity soils during recent years. However, an increasing interest has been dedicated to concrete.

Corrosion of reinforced concrete can be arrested by employing cathodic protection. The California Department of Transportation pioneered the use of impressed-current cathodic protection (ICCP) in the 1970 [23]. Sacrificial anode cathodic protection systems have been employed as part of a cathodic protection system applied to pilings in Lake Maracaibo, Venezuela ≡24].

Laboratory evaluations were conducted on Al anodes that could be used for sacrificial cathodic protection of reinforced concrete≡16∂. Anodes were fabricated into test coupons and coupled to small lengths of reinforcing steel. The Al-steel couples were placed in simulated concrete environments, which consisted of sealed containers filled with silica sand treated with a chloride solution. The treated sands were dried to obtain resistivities of 1600, 4190 and 7500 6-cm. The results obtained showed that Al could be an alternative for employment as a galvanic anode in reinforced concrete in a wide spectrum of resistivity.

1.2 Magnesium anodes. Dissolution mechanism of Mg sacrificial anodes under electrochemical testing [16,25,30].

The electrochemical behaviour of magnesium galvanic anodes under ASTM Test Method G 97-89 [25,26] conditions was investigated by measuring electrochemical impedance. Mg rods machined from a sample of commercial anode are used as anodes (working electrode), while a piece of steel pipe, which served also as the electrochemical cell (cathode test pot) are used as cathodes (counterelectrodes).

Samples were held galvanostatically at 0,039 mA/cm^2 until electrochemical impedance spectroscopy (EIS) testing was completed. All samples were held potentiostatically during the test. Closed-circuit test specimen potential was obtained daily, before and after EIS testing.

EIS measurements were used to monitor the corrosion process on the magnesium daily for the duration of the 14-dayf test. The magnesium anode potential was measured daily, and was seen to undergo a change from -1,610 mV (sce) to -1,680 mV (sce). Figure 3 gives the characteristic impedance spectra obtained during immersion of the magnesium anode in the solution (for 14 days at 20°C, always showing two loops). To interpret impedance results, a model was established [25] that included the electrolyte resistance, the parts of the impedance corresponding to the corrosion product film (hydroxide layer) formed, and the impedance of the interface. The model was proposed according to

the reported behaviour of magnesium ([27,28,29] and was validated by comparing its results to the real condition of the magnesium anode.

According to this model, the electrochemical impedance of magnesium anode was given by:

$$\frac{1}{Z - R_s} = \frac{1}{\frac{1}{\frac{1}{C_{dl}} + \frac{1}{R_1}} + \frac{1}{\frac{1}{C_{pol}} + \frac{1}{R_{po}}}}$$

The spectra analysis showed the capacitance of a corrosion porous layer (C_{po}) in the high-frequency (HF) region and double-layer capacitance (C_{dl}) in the low-frequency (LF) region. The resistive component of the corrosion porous layer (R_{po}) in the frequency range between 100 Hz and 1000 Hz, and the resistance of charge-transfer reaction (R_t) was in the LF region.

To interpret the impedance diagrams, equivalent circuit models were used. The behaviour of the magnesium-electrolyte interface could be described by the proposed model with the electric equivalent circuit that corresponds to the porous film model or two-layer model [25], which was used to successfully reproduce all the impedance spectra obtained. According to this model, the impedance diagram might bring into view two semicircles. The HF semicircle is usually attributed to the porous film, whereas the lower frequency semicircle corresponds to the charge transfer reactions or faradic process.

C_{po} decreased with time whereas both R_{po} and R_t increased with time [25]. This increase in protection with immersion time provided evidence for the existence of a protective layer over the magnesium surface, one of $Mg(OH)_2$.

C_{po} of the layer could be described by:

$$\frac{C}{A} = \varepsilon\varepsilon_0 \frac{1}{d}$$

Where ϵ is the dielectric constant, ϵ_0 is the permitivity in free space (8.854×10^{-12} F/m). C/A is the capacitance per unit area, and d is the thickness. Thus, as the thickness of the $Mg(OH)_2$ increases, C is expected to decrease for the C_{po} value.

Since the resistance of a film is proportional to its resistivity and thickness, an increase in R_{po} was interpreted to mean that passivation of the $Mg(OH)_2$ layer increased with immersion time.

Analysis of the corrosion products formed on the magnesium anode and precipitated in the solution was carried out and the presence of $Mg(OH)_2$ seemed clear for the corrosion products on the magnesium anode. A visual and microscopic inspection of the magnesium electrode did not show any localised corrosion after the test.

In the results obtained, the magnesium anode did not corrode locally and charge transfer occurred uniformly underneath the oxide.

1.3 Zinc Anodes. EIS testing of thermal spray Zn anodes for concrete applications [31-33]

The use of sacrificial zinc anodes for cathodic protection (CP) of steel in reinforced concrete is a subject of increasing interest, especially regarding potential applications on highway bridges seriously damaged by chloride contamination. One anode material gaining acceptance is thermally sprayed zinc (TSCP).

The feasibility of using EIS, as a monitoring tool to determine whether CP level is sufficient to mitigate corrosion was investigated for carbon steel in concrete [31,32]. As a first approach, this investigation deals with the behaviour of the galvanic couple steel/zinc under CP conditions in NaCl solution. The EIS diagrams obtained were compared with those corresponding to laboratory concrete samples, whose surface was thermal sprayed with Zn. [33]

The California Department of Transportation pioneered the use of thermal-sprayed Zn anodes for existing structures damaged by corrosion in 1982 [34]. This tecnology has since been employed in a number of large projects such as bridge structures. In Mexico this tecnology is known, but has not yet been applied.

In recent years, the cost of rehabilitating and protecting bridges with CP has fallen by as much as one half. Actually, there are more than 500 bridges in North America with installed CP systems [35]. Of the more than 575,000 bridges in the National Bridge Survey, it is estimated that 44% are in need of repair [36].

With the object of contributing to a better knowledge of the factors afecting these systems' efficiency and yield, laboratory assays have been carried out to gather information on the behavior and mechanism of Zn/concrete interphase and especially of the galvanic couple Fe/Zn, which is responsable for galvanic cathodic protection.

Potentials for the Zn anode were measured with respect to the steel cathode. Figure 4 shows results of the potential of a steel cathode as a function of immersion time. Throughout the experiment, the steel cathode remained at potential values more negative in value than -800 mV (SCE), maintaining the steel protected.

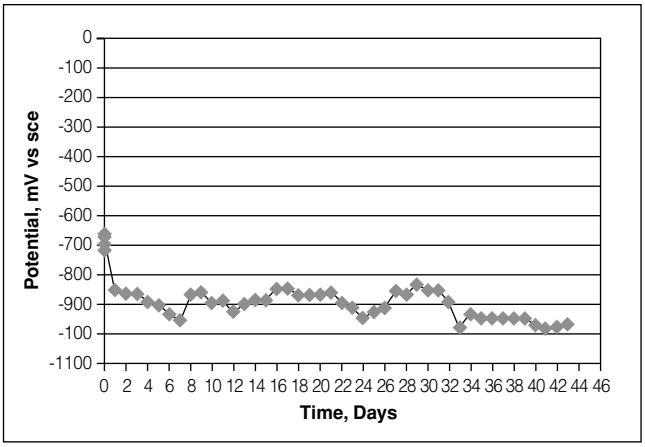

Figure 4. Potential of cathode (steel) as a function of time during cathodic protection of reinforced concrete by thermal spray Zn-anode.

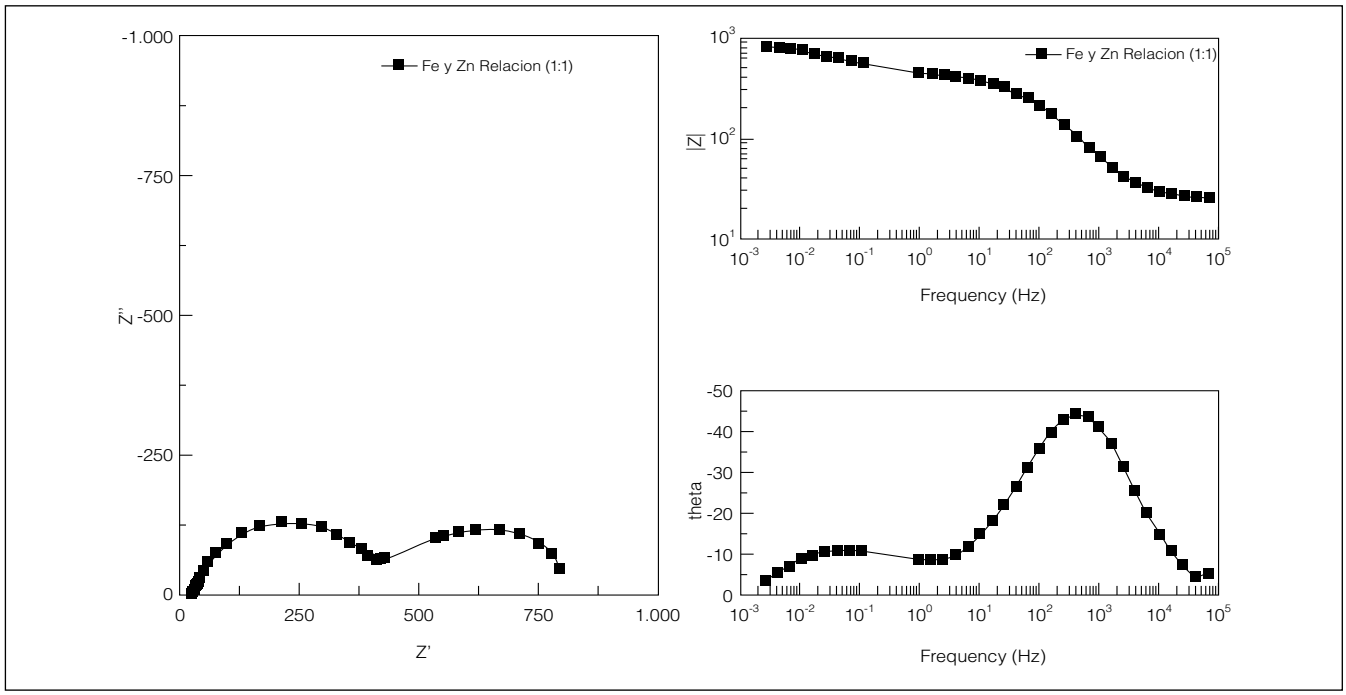

Figure 5. Impedance diagrams of the galvanic couple Fe-Zn in 3% NaCl [33].

All the Bode impedance diagrams (phase angle vs. frequency) obtained during the experimentation time [33] show the presence of a peak at about 100 - 200 Hz, which could correspond to Zn, and a second peak at lower frequencies, corresponding to Fe. The measured potentials on steel cathode corresponding to the same days were -1032 and -896 mV (SCE), both of them characteristic of protection of Fe by the Zn anode.

To confirm these results, EIS experiments were carried out with the galvanic couple Fe/Zn in the same NaCl solution. The impedance diagrams corresponding to steel, Zn and steel-Zn in NaCl solution at the corrosion potential value were obtained. The Nyquist diagrams show capacitative semicircles and for the particular case of the galvanic pair Fe- Zn with a ratio area of 1:1, two semicircles. The presence of two constant times seems to be clear, as verifiable in the corresponding phase angle diagram. The value of f_{max} is of 4 Hz for steel, 300 Hz for Zn, and for the galvanic couple Fe-Zn, a detailed analysis of which is presented in Figure 5. The presence of two peaks at 400 Hz and 30 mHz, that could correspond to Zn and Fe respectively, are clearly shown.

The behavior of the galvanic couple can be explained by means of the equivalent electrical circuit. In this electric circuit, the solution resistance will be in series with two parallel RC circuits. The results obtained modeling with this circuit [33] show a good agreement with experimental results. The phase angle diagram as a function of frequency permits corroboration that the pair Fe-Zn initially shows a behavior characteristic of steel. But from the third day the behavior is mixed (Zn dissolution to protect Fe) and for the fourth day the predominance of Zn is clearly shown.

2. Improving electrochemical efficiency of Mg anodes [37-43]

Mg anodes currently have limited offshore use. Alloys of Mg are particularly suited for high resistivity environments where their inherent negative potential and high current output per unit weight is considerable. The theoretical half-cell potential of Mg is -2.37 V (NHE) or -2.12 V (SCE). However, the practical measurement of magnesium anode potential is considerably more noble. The AZ63A anode (nominal 6% Al and 3% Zn) has a potential of -1.48 V (SCE), while the proprietary Galvomag anode containing high purity magnesium with 0.9 - 1.2 % added Mn and controlled impurities has a solution potential of -1.68 V (SCE).

Aside from the large difference observed between theoretical and measured solution potentials, magnesium anodes generally have a current efficiency less than other galvanic anodes. The theoretical current yield of a magnesium anode is approximately 2200 A-h/kg. The practically observed current efficiency rarely exceeds 50%.At least three areas are known to contribute to the factor responsible for the low current efficiency and more-noble-than theoretical solution potential of the magnesium anode [25,44].

- Anolyte chemistry. Changes in anion and cation concentration, which occur close to the dissolving magnesium surface and the effect that these ions have on behaviour.
- Anode alloying elements and structure. Alloying elements and thermal story attendant with casting affect the structure, which are in turn related to filming characteristics and local-cell action.
- Anodic electrochemistry.

Studies on factors responsible for the low current efficiency in magnesium anodes, including changes in anion and

cation concentration which occur close to the dissolving magnesium surface and the anodic electrochemistry, have been carried out in the past [45,46].

The composition of the magnesium anode is known to affect its current capacity, solution potential and efficiency. Many alloying elements have been used in order to improve the properties of magnesium anodes [43,44].

As has been pointed out in the past, the metallurgical features of Mg sacrificial anodes such as casting conditions and heat treatment are closely related to anode operation potential and also to their own efficiency. In the magnesium type of anodes, contrary to the requirements for anode materials, corrosion occurs by pitting rather than by uniform corrosion. This corrosion characteristic shifts the potential to more electronegative values [46]. For instance, magnesium suffers pitting when it is exposed to chloride solutions in nonoxidizing media at open circuit potentials [47]. The deleterious effects of Ni, Fe and Cu in Mg anodes are well-documented [48].

In order to investigate the main reasons for low current efficiency of the commercial magnesium sacrificial anodes, a study was carried out with the main objective of correlating the microstructure characteristics and the alloying elements of the magnesium anodes with their efficiency. Heat treatment effects on the current efficiency of commercial Mg anodes was also studied [38,43].

Figure 6 shows a micrograph of the structure obtained by gravity casting of commercial magnesium into a copper mould. As can be observed, the microstructure in all the ingots was of the cellular type. Cell size in ingots varied between 5 μm in the centre of the ingot to above 10 μm in the outer region of the ingot. The microstructure mainly consists of cells of α-Mg, but few precipitates were observed at cell boundaries. Because the magnesium ingots were produced in order to assess their behaviour as magnesium sacrificial anodes, a heat treatment was performed at 300 °C for eight hours. Figure 7 shows the microstructure observed in all the specimens, which consists mainly of equiaxed grains. Inside these grains a cellular structure was observed and these cells were nearly free of precipitates.

Microanalyses were carried out in order to quantify how the microstructure was modified by the chill casting technique and the heat treatment of specimens, before performing the evaluation of magnesium sacrificial anode test, in terms of the nature of impurities like copper, iron and nickel.

In the as-cast magnesium ingots and especially in regions where the precipitates were present, the microanalysis system detected precipitates rich in iron (shown in Figure 6) and a uniform concentration of copper, iron and nickel in solid solution with some major concentration of iron at grain boundaries.

Figure 6. Cellular microstructure obtained by gravity casting commercial magnesium into a cylindrical copper mould. Second phase particles were detected as Fe/rich particles [43].

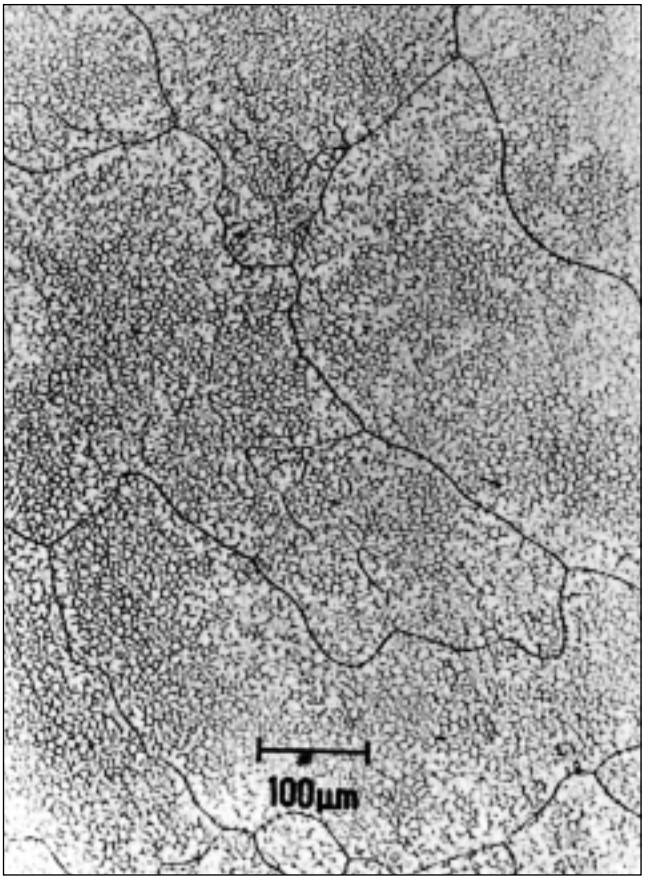

Figure 7. Equiaxed grain structure of a magnesium sacrificial anode after heat treatment (300 °C, 8 hrs). Inside the equiaxed grains, a cellular microstructure is observed with nearly free precipitates [43].

Microanalyses of the magnesium ingots with heat treatment revealed small iron-rich precipitates and a layer of aluminium-rich second phase of about 0,05 μm in thickness was detected at grain boundaries.

The efficiency values for sacrificial anode specimens in the ascast condition are superior to 50% and with heat treatment, the efficiency values are close to 70% [43].

After evaluation of the magnesium sacrificial anode, the surface of specimens was observed. Figure 8 shows the microstructure of magnesium in the as-cast condition after evaluation of its efficiency. As can be seen, corrosion of magnesium occurs preferentially in regions rich in second phase Fe-rich precipitates, which were located at cell boundaries. Corrosion in these regions is by pitting, forming a step-like pattern.

Figure 9 shows the observed microstructure of the magnesium sacrificial anode with heat treatment after the test. The corrosion features are more uniformly distributed compared to specimens without heat treatment, and corrosion was of the uniform type.

Heat treatment effect on commercial magnesium anodes was also studied [38,42,43]. By using specific heat treatments [42] the efficiency of the Mg anodes was improved, which made it possible to control the amount and size of the precipitates and of the second phase particles localised at grain boundaries and inside the matrix.

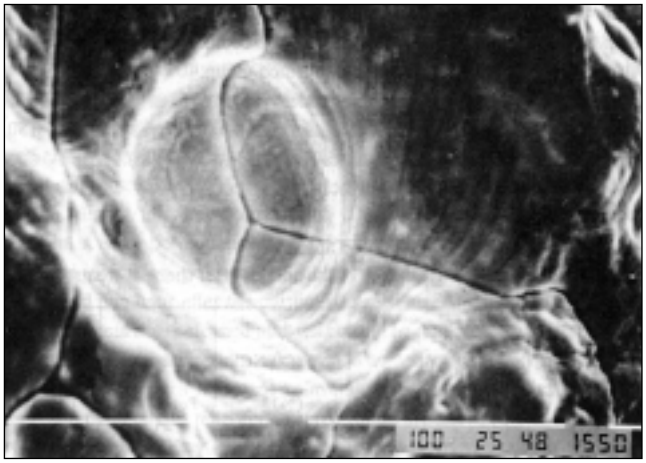

Figure 8. Microstructure of magnesium in the as-cast condition after the evaluation test, in which pitting of the corrosion pattern can be observed [43].

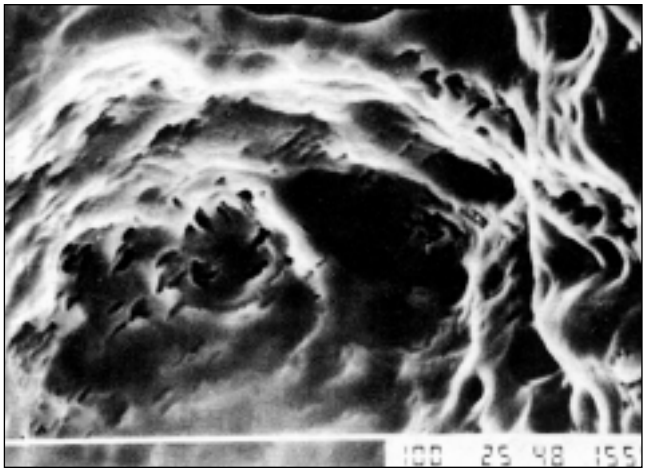

Figure 9. Microstructure of magnesium in the as-heat treated condition after the evaluation test. Corrosion is more uniform as compared to the as-cast magnesium [43].

Lower anode efficiency was related to the presence of Mnrich second phase particles where corrosion occurs along a narrow region in the grain boundaries. In order to produce high efficiency of Mg-anodes it is necessary to control the impurities that are uniformly distributed in solid solution, and other microstructural parameters such as grain size. The solution could be to use alternative casting processes [37] and heat treatments [39,41].

3. Design and development of new Al-alloy anodes In/Hg free.

3.1 Introduction

Presently, the most commonly employed sacrificial metals for cathodic protection systems are alloys of magnesium (Mg), zinc (Zn) and aluminium (Al). The Al-anodes are closely related to alloy chemistry and to environmental application. Aluminium has attained considerable merit as the basis for a galvanic anode mainly due to its low density, large electrochemical equivalent, availability and reasonable cost. The low electrode potentials of Al-anodes are readily adaptable to a variety of saline environments such as seawater, marine muds and brackish waters. Unalloyed-Al adopts a relatively noble solution potential in saline media as a result of its protective oxide film. The oxide is the cause of rapid polarization when aluminium is placed under a corrosion load in a cathodic protection circuit. Nevertheless, the success of the Al-anode depends upon the alloying of certain metals whose surface role is to ultimately prevent the formation of a continuous adherent and protective oxide film on the alloy, thus permitting continuous galvanic activity of the Aluminium. Research carried out towards the development of Al-alloys appropriate for cathodic protection has considered the influence of alloying elements such as Zn, titanium (Ti), mercury (Hg), and indium (In) (see, for example Ref [49,50]). The employment of each of those elements has shown an improvement of Al-activation in neutral chloride media. However, the seemingly good results obtained in this field are in contrast with the increased sensitivity to environmental protection. Particularly the use of In alone or coupled with Hg in Al-alloys during dissolution results in sea life pollution and gives rise to great environmental issues. In order to avoid sea life pollution due to elements such as Hg and In, and at the same time providing an Al-alloy adequate for cathodic protection application, the Al-Zn-Mg system has been investigated in terms of distribution of intermetallics in the α -Al matrix capable of breaking down passive films as well as presenting good electrochemical efficiencies [51].

For instance, reports have been made [52], in the as-cast condition, of the existence of a microstructure consisting of α -Al solid solution with precipitation of the τ -phase and an eutectic consisting of a fine dispersion of the $\alpha + \tau$ segregat-

ed at grain boundaries. Further dispersion of the τ phase in the matrix was increased by means of thermal treatments applied to as-cast ingots, by taking advantage of the fast kinetic reactions occurring in solid state at 400°C, giving as a result Al-anodes with electrochemical efficiencies up to 78% [53].

The main purpose of this research is to identify the possibility of the substitution of Al-Zn-In and Al-Zn-In-Hg sacrificial anodes, by alloys of the Al-Zn-Mg type, in order to avoid sea-life pollution without decreasing current efficiency of the resulting anodes. The first part of this research was focused on the identification and distribution of precipitates in the Al-alloy, in order to achieve two goals; the first one is to obtain a good surface activation of the anode; the second, to yield corrosion products similar to those found in sea water in order to avoid pollution of sea life. As a first step reference was made of the work of Barbucci et al. [53] producing Al-Zn-Mg alloys but with additions of Li. The resulting microstructure was then characterized, with particular attention to identification of precipitates in the α -Al matrix and eutectics in interdendritic regions, in both as-cast ingot and aged samples. The research was also directed towards the effect of Li additions on superficial activation of the anode by means of precipitation of the δ -AlLi intermetallic at grain boundaries and/or matrix, and taking advantage that the Zn decreases the solid solubility of Li in the α -Al phase [54].

3.2 Experimental Procedure

An Al-5 at. % Zn-5 at. % Mg-0.1 at. % Li alloy was prepared with commercially available Al, Zn and Mg with purities of 99.98 %. Li was used as a wire of 3.2 mm in diameter and 99.9% of purity with 4.5 mg/cm of Sodium (Na). Due to previous experiences during melting of this kind of alloys and in order to avoid losses of Mg, Zn and Li, these elements were placed in Al-capsules. Initially, the Al was placed in an alumina/graphite-coated crucible and melted in a resistance furnace under an argon atmosphere. Once the Al was melted, the liquid bath was overheated 150ºC and the Al-capsules containing Zn and Mg were added. The bath was stirred with argon for 10 minutes in order to achieve uniform distribution of Zn and Mg. Immediately after this operation, the Al-capsule containing Li was added to the liquid bath, which was stirred with a flux of argon for another 5 minutes after which the liquid alloy was poured into a copper mold of dimensions 8x8x50 cm.

In order to perform the characterization of the resulting microstructure, the ingots were sectioned transversally to the heat flow, ground, polished and etched in Keller's reagent to reveal the different phases, precipitates and/or intermetallic compounds present in the ingot. Aged treatments were performed in the as-cast ingot in order to enhance precipitation, following to aging steps: 1) aging at 400°C for 5 hours, and 2) aging at 400°C for 5 hours with an additional heating of 160°C for 2 hours. The resulting microstructure was characterized using a Stereoscan 440 scanning electron microscope (SEM) and a 2100 Jeol scanning transmission electron microscope (STEM). Both electron microscopes were equipped with WDS-microanalyses facilities. X-ray diffractometry on aluminium samples in all conditions using a Siemens 5000 X-ray diffractometer using a Cu Kα radiation, a Ni filter and a scan velocity of 2°/min.

3. 3 Results and discussion

A representative microstructure observed in the as-cast ingot as shown in Figure 10, consisted of α -Al dendrites with sizes between 130 to 150 μ m. In the interdendritic regions, the presence of a eutectic and black spherical particles was observed. The eutectic showed a white color with a maximum width of 10 μm, always following the contour of the dendritic arms. This eutectic, instead of presenting platelet morphology, like that reported by Barbucci et al. [53] showed the presence of rows formed by gray spherical particles.

Figure 11 shows the microstructure observed in samples aged at 400°C (5 hr). The dendritic structure was modified, giving rise to the coarsening of primary and secondary arms. The white eutectic (with a maximum with of 7 μ m) started to migrate towards future grain boundaries, leaving traces of the interdendritic species in the α -Al matrix, which

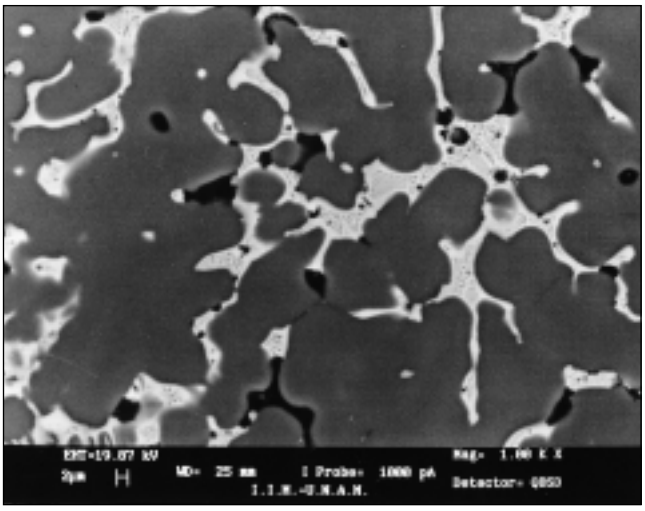

Figure 10. As-cast microstructure of the Al-Zn-Mg ingot.

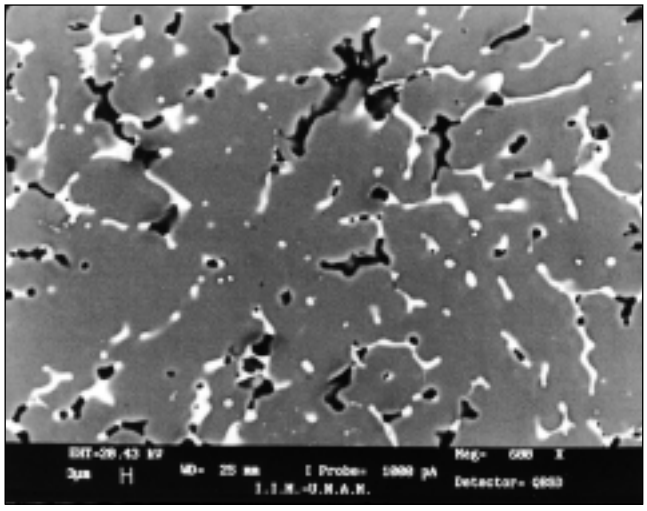

Figure 11. Microstructure observed in samples aged at 400°C (5 hr).

takes the morphology of spherical particles. Also, it was observed that the spherical particles which were present as rows inside the white eutectic, started to growth. The black spherical particles located at secondary dendritic arm spacing did not show any change at this stage.

In order to evaluate the effect of a secondary aging treatment, the samples aged at 400 ºC for 5 hours received an additional aging treatment a 160 ºC for 2 more hours. The observed microstructure under this aging condition is shown in Figure 12, where there appears to be an increase in the quantity of black spherical particles following the contours of the secondary dendritic arms. The width of the space occupied by the black spherical particles increased from 2 μ m (in the as-cast ingot) to (6 μ m (in this aging stage).

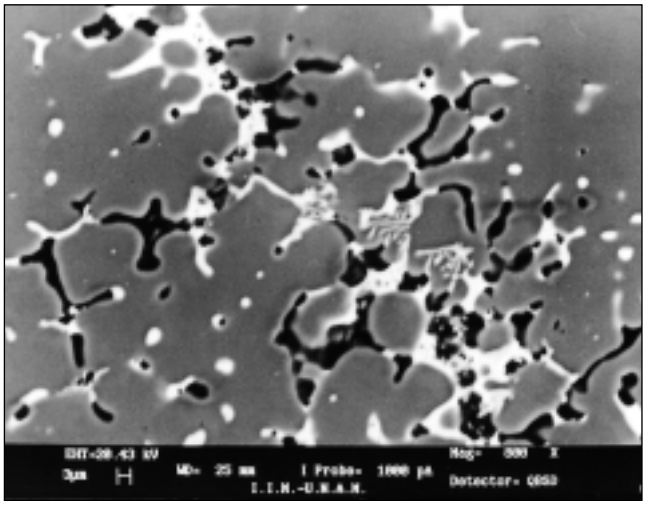

Figure 12. Microstructure observed in samples aged at 400ºC (5 hr) with an additional heating of 160 °C (2 hr).

In order to qualitatively identify the species present in the as-cast ingot and in the aged specimens, X-ray diffractometry was applied and from the collected data, seven peaks were detected in each condition. As expected, the main peaks corresponded to the α -Al phase. Also, the presence of binary precipitates of MgZn, Mg_4Zn_7, Mg_7Zn_3, $MgZn_2$, AlMg, Al_3Mg_2, $Mg_{17}Al_{12}$, Al_4Li_9, LiZn, AlLi were detected; ternary precipitates of $AlMg_4Zn_{11}$, Al_2MgLi, LiMgZn, $Al_2Mg_3Zn_3$ and quaternary precipitates of $Al_{0.9}Li_{34.3}Mg_{64.5}Zn$ and $Al_{0.9}Li_{34.3}Mg_{64.5}Zn$ also appeared. The kind of precipitates and their respective d-spacing are shown in Table 1.

An interesting feature of these X-ray diffractograms was an increase in the relative intensity (I/I_0) of peaks II, III and VII for both aged conditions, indicating, from a qualitative point of view, the precipitation of particles containing Li.

In addition, WDS-microanalyses were carried out in specimens in both as-cast and as-aged conditions (see Table 2). For example, in the as-cast specimens, it was possible to retain 4,7 at.% Zn and 4,2 at. % Mg in α -Al solid solution. Li was not detected due to the characteristics of the detector.

Table 2. WDS results of microanalyses of as-cast and aged specimens (in at. %)

Condition (→) *Microstructure* (↓)	*As-cast* *(at. %)*	*Aged*1* *(at. %)*	*Aged*2* *(at. %)*
α -Al dendrites Al	91.00 ± 2.0	---	---
Mg	4.20 ± 0.50	3.50 ± 0.50	3.50 ± 0.10
Zn	4.70 ± 0.20	3.22 ± 0.65	4.00 ± 0.15
White eutectic Al	41.00 ± 3.0	39.00 ± 4.0	41.00± 3.0
Mg	32.00 ± 1.0	33.00 ± 2.0	32.00± 2.5
Zn	27.00 ± 3.0	28.00 ± 1.5	27.00± 3.6
Black particles Al	---	---	---
Mg	71.00 ± 2.0	72.00 ± 2.5	70.00 ± 4.00
Zn	29.00 ± 6.0	28.00 ± 4.0	29.00 ± 2.00

*1 aged at 400ºC, 5 hr, *2 aged at 400ºC with an additional heating of 160 °C for 2 hr.

In the first as-aged condition (400°C, 5 hr), the amount of Zn and Mg present in the α -Al solid solution decreased. This decay in both elements was attributed to the coarsening of the eutectic located in interdendritic regions. Regarding composition of this eutectic, the amount of Zn detected was ranged from between 32 to 33 at. % and the amount of Mg was in the range between 27 to 28 at. %, the remaining being Al. As mentioned before, the black spherical particles observed in the interdendritic regions did not present any change, and their composition was almost constant, corresponding to precipitates of Mg_7Zn_3. In the second aging stage an increase in the quantity of black particles in the interdendritic region was observed, with an almost constant composition. The only detected change in composition cor-

Table 1 Phases and compounds identified by X-ray diffraction

Peak	*As-cast*		*Aged*1*		*Aged*2*		*Phases*
	d(Å)	I/I_o	*d(Å)*	I/I_o	*d(Å)*	I/I_o	
I	2.340	100	2.334	100	2.344	100	α -Al, MgZn, Mg_4Zn_7, Mg_7Zn_3, AlMg, Al_3Mg_2, Al_4Li_9, $AlMg_4Zn_{11}$
II	2.028	19	2.023	53	2.028	35	α -Al, $AlMg_4Zn_{11}$, Al_2MgLi
III	1.434	44	1.432	49	1.435	54	α -Al, MgZn, $MgZn_2$, $Mg_{17}Al_{12}$, LiZn, LiMgZn, Al_3Mg_2
IV	1.224	38	1.223	38	1.224	14	α -Al, AlMg, AlLi
V	1.172	5	1.171	4	1.172	4	$Al_{0.9}Li_{34.3}Mg_{64.5}Zn$
VI	0.932	6	0.932	12	0.932	5	α -Al, $Al_{0.7}Zn_{0.3}$, $Al_2Mg_3Zn_3$
VII	0.908	4	0.906	19	0.906	12	AlLi, $Al_{0.7}Zn_{0.3}$, $Al_{0.9}Li_{34}Mg_{64}Zn$, $Al_2Mg_3Zn_3$

*1 aged at 400ºC, 5 hr, *2 aged at 400ºC with an additional heating of 160 °C for 2 hr.

responded to the transition of the eutectic to a dendrite-like precipitate, whose composition corresponded to Al-16,6 at. % Zn-13,25 at. % Mg with a contamination of 3,3 at. % Fe.

TEM observations performed in the specimens with and without heat treatment identified the presence of a platelet-like precipitate of about 1,800 nm in length and spherical precipitates (40 to 200 nm. Selected area diffraction patterns taken in those precipitates identified them as the intermetallic τ -$Al_2Zn_3Mg_3$, Mg_7Zn_3 and δ -AlLi (80 nm).

Regarding the electrochemical behavior in terms of efficiency of the as-cast ingot and aged samples, it can be said that the efficiency on the as-cast ingot showed an average value of 62%, while the efficiency in aged samples at 400ºC (5 hr) showed an average value of 67%, and the aged sample at 400°C for 5 hours with an additional heating of 160°C for 2 hours, showed an average value of 65%.

Recent research directed towards the development of aluminium sacrificial anodes of the Al-Mg-Zn type, reported ≡53∂ values of electrochemical efficiency between 63 to 78% (-1,082 mV; SCE). These results were attributed to a good dispersion of the τ -phase [55] in the α -Al matrix, which was reached by a long-term aging treatment (400ºC, 24 hr). The intermetallic compound was shown to be responsible for the breakdown of the passive film and at the same time to lead to a quite generalized dissolution. When additions of In, gallium (Ga) and calcium (Ca) were made into the Al-Mg-Zn alloy ≡56∂, and the resulting alloy was thermally treated at 500ºC (4 hr), the Al-anodes reached efficiencies up to 95.6% (-1090 mV; SCE). This excellent efficiency value was attributed to a homogeneous distribution of Ga and a precipitation of In and Ca. Therefore, research has shifted to the production of Al-alloys which can show high electrochemical efficiencies. To attain that goal, during the present research it was observed that the as-cast microstructure must be improved in order to increase the electrochemical efficiency of Al-anodes by means of decreasing or eliminating the presence of Mg_7Zn_3 precipitates in interdendritic regions. Moving in this direction is due to the fact that during dissolution of the Al-anode, the Mg_7Zn_3 particles did not dissolve. This provoked the isolation of some α -Al dendrites, giving place to a localized pitting corrosion mechanism and at the same time decreasing the electrochemical efficiency of the Al-anode. On the other hand, it was detected that precipitates of the τ -$Al_2Zn_3Mg_3$ and δ -AlLi type, played an important role in terms of breaking down the aluminium oxide passive film, simultaneously permitting a continued galvanic activity and an increase the electrochemical efficiency of the Al-anode.

3.4 Conclusions

1. The resulting Al-Zn-Mg-Li alloy showed two kinds of species in the interdendritic spacing. These corresponded, to a eutectic of $Al_2Zn_3Mg_3$ and precipitates of Mg_7Zn_3.

2. By means of TEM observations, the presence of the τ -$Al_2Mg_3Zn_3$ intermetallic compound, precipitates of Mg_7Zn_3 and δ -AlLi precipitation in the α -Al matrix were identified. The presence of those species for the activation of the aluminium electrode were found relevant by means of passive film breakdown which can lead to a quite generalized dissolution of the Al-anode.

3. In order to improve the electrochemical efficiency of the Al-anode, it was apparent that research must be focused on the role played by the τ -$Al_2Zn_3Mg_3$, Mg_7Zn_3 and δ -AlLi compounds in the α -Al matrix, and on the effect of the decay of eutectic and particles in interdendritic regions. This will result in the prevention of the formation of a continuous, adherent and protective oxide film by particle precipitation, leading to a uniform dissolution of the Al-anode.

References

[1] Ashworth, V. (1986). The theory of cathodic protection and its relation to the electrochemical theory of corrosion in Cathodic Protection: Theory and Practice, V. Ashworth and C.J.L. Booker Editors, Ellis Horwood Ltd., Chichester, England, p. 13-30.

[2] Peabody, A.W. (1967). Control of Pipeline Corrosion, NACE, Houston.

[3] Parker, M.E. and Peattie, E.G. (1984). Pipeline Corrosion and Cathodic Protection, Third Edition, Gulf [JG2][JG3]Publishing Co., Houston.

[4] Morgan, J.H. (1987). Cathodic Protection, Second Edition, Nace International, Houston.

[5] von Baeckmann W., Schwenk, W. and Prinz, W. Editors, (1997), Handbook of Cathodic Corrosion Protection. Theory and Practice of Electrochemical Protection Processes, Third Edititon, Gulf [JG4][JG5][JG6]Publishing Co., Houston.

[6] Code of Practice CP1021, Cathodic Protection, BSI[JG7], London (1973),

[7] NACE RP 01-69, Control of External Corrosion on Underground or Submerged Metallic Piping Systems, NACE, Houston [JG8](1969),

[8] Avila, J. and Genescà, J. (1991). Mas Alla de la herrumbre II. La lucha contra la corrosión, FCE, México D.F[JG9].

Genescà, J. (1993) «Anodos galvánicos en protección catódica. Factores que afectan su eficiencia comportamiento» *Memoria del Seminario Internacional Agencia Internacional de Cooperacion del Japon (JICA) Instituto Politecnico Nacional*. (*IPN)*, Villahermosa, 11 Marzo.

Bertancourt, L., Rodriguez, C., Genescà, J. (1993), «Ensayos normalizados para ánodos galvánicos de magnesio». *Memorias del XIX Congreso Academia Nacional Ingeniería*, Acapulco, 24 Septiembre. pág. 163-167.

Genescà, J. (1994), «Cathodic Protection Criteria for Buried Steel Pipeline». *Memorias de las conferencias del III Seminario México-Japón´94.* Materiales de acero para tuberías para la industria petrolera. IPN-JICA. 19-21 Enero. México D.F.. pag. 6.1 a 6.12.

[9] Hoar, T.P. (1968)

[10] Avila, J. and Genescà, J. (1989), Mas alla de la herrumbre, Col. La Ciencia desde México, Fondo Cultura Económica, México D.F.

[11] Bennett, L. H[JG10]. (1978), Economic Effects of Metallic Corrosion in the US, NBS Special Publication 511-1, Washington DC.

[12] Jensen, F. (1979). Testing of Sacrificial Anodes - Necessity and Experience, Trans. I. Mar. E (C), Vol. 91. Conference No. 1, paper C14, 86-100.

[13] Standard Test Method «Impressed Current Laboratory Testing of Aluminum Alloy Anodes», NACE Standard TM0190-98. NACE International, Houston, 1998.

[14] DNV Recommended Practice RP B401 (1993): «Cathodic Protection Design», Det Norske Veritas Industry AS, Hovik 1993.

[15] Suárez, M., Rodriguez, C., Rodriguez, F.J., Juárez, J. and Genescà, J., (1999), EIS testing of an indium activated aluminium alloy sacrificial anode using DNV RP B401, EUROCORR'99. Simposium: Marine Corrosion. Dechema, Frankfurt, p.1-9.

[16] Genescà, J., Betancourt, L., Jerade, L., Rodriguez, C. and Rodriguez, F.J. (1998), «Electrochemical Testing of Galvanic Anodes» in *Electrochemical Methods in Corrosion Research VI*. Ed. Pier Luigi Bonora and F. Deflorian, *Materials Science Forum*, Vols. 289-292, pp. 1275-1288, ISBN # 0-87849-819-2, Trans Tech Publications Ltd, Uetikon-Zuerich, 1998.
Espelid, B., Schei, B. and Sydberger, T. (1996). Characterisation of sacrificial anode materials through laboratory testing, Corrosion '96. Nace International, Houston.

[17] Attanasio, S.T., Murray, J.N. and Hays, R.A., (1996), Non-Uniform Electrochemical Behavior of Indium-Activated Aluminum Alloy Anodes, Corrosion/96, NACE International, Houston , Paper No. 546.

[18] Hine, R.A. and Wei, M.W., (1964), Mat. Prot. 3, 11, 49.

[19] Lye, R.E., (1990), Mat. Perf. 29, 5, 13.

[20] Uruchurtu, J. (1991), Electrochemical Investigations of the Activation Mechanism of Aluminum, Corrosion 47, 6, 472-479.

[21] Reboul, M.C., Gimenez, P. and Rameau, J.J., (1983), A Proposed Activation Mechanism for Al-Zn-In Anodes, CORROSION/83, NACE, Houston , Paper No. 214.

[22] Murray, J.N., Hays, R.A. and Lucas, K.E., (1993), Testing Indium Activated, Aluminum Alloys Using NACE TM0190-90 and Long Term Exposures, CORROSION/93, NACE, Houston , Paper No. 534.

[23] Whiting, D.A., Nagi, M.A. and Broomfield, J.P. (1996), Laboratory evaluation of sacrificial anode materials for cathodic protection of reinforced concrete bridges, Corrosion (52) 6, 472-479.

[24] Rincon, O.T., Carruyo, A.R., Romero, D. and Cuica, E. (1992), Evaluation of the Effect of Oxidation products of Aluminum Sacrificial anodes in Reinforced Concrete Structures, Corrosion 48 (11) 960-966.

[25] Genescà, J., Betancourt, L. and Rodriguez, C., (1996) «Electrochemical Behavior of a Magnesium Galvanic Anode under ASTM Test Method G 97-89» *Corrosion (NACE)* 52 (7) 502-507.

[26] ASTM Test method G 97-89, (1989), «Standard Test Method for Laboratory Evaluation of Magnesium Sacrificial Anode Test Specimens for Underground Applications» 1989 Annual Book of ASTM Standards, vol. 03.02, West Conshohocken, PA. ASTM. P. 377-380.

[27] Casey, E.J. and Bergeron, R.E., (1953), Can. J. Chem. 31, 849.

[28] Perrault, G.G., (1970), J. Electroanal. Chem. 27, 47.

[29] Straumanis, M.E. and Bathia, B.K., (1963), J. Electrochem. Soc. 110, 357.

[30] Betancourt, L., Lee, J.C., Rodriguez, C. y Genescà, J., (1995), «Comportamiento electroquímico del Magnesio como ánodo galvánico». *AFINIDAD* 52 (458) 258-266.

[31] Talavera, M.A., Pérez, J.T., Pérez, T. y Genescà, J. (1999), «Seguimiento por impedancia electroquímica de la protección catódica del acero por ánodos galvánicos de zinc», Memorias Congreso Sociedad Mexicana Electroquímica, SME´99, trabajo # 13, pag. 13/1 a 13/11. Mérida.

[32] Pérez, J.T., Talavera, M.A., Castro, P., Genescà, J., (1999), «Protección catódica del acero de refuerzo en concreto mediante zinc aplicado por rociado térmico»., Memorias V Congreso Iberoamericano de Patología de las Construcciones, CONPAT´99, Montevideo. Tomo III. Pag. 1533-1540. ISBN 9974-39-193-8.

[33] Talavera, M.A., Perez, T., Castro, P. and Genescà, J., (2000),»EIS Measurements on Cathodically Protected Steel in Concrete», *NACE Corrosion'2000*. Houston, Paper # 794. Pag. 794/1-794/9.

[34]. «The First Zinc-Anode CP System - 11 Years Later «, Concrete Repair Digest (1994): p.292.

[35] Jackson, D. «Cathodic Bridge Protection is More Affordable than Ever», Focus, September (1997): p.5.

[36] Burke, P.A. Materials Performance 33,6(1994):p.48.

[37] Juárez, J., Martinez, L. and Genescà, J. (1993). «Solidification Techniques and Electrochemical Properties of Magnesium Base Anodes» Corrosion'93. Paper No. 536. NACE, Houston.

[38] Juárez, J., Genescà, J and Pérez, R., (1993), «Improving the Efficiency of Magnesium Sacrificial Anodes», *Journal of the Minerals, Metals and Materials Society* 45 (9) 42-44.

[39] Salas, G., Noguez, M.E. and Genescà, J., (1994), «Cooling rate effect in the ascast magnesium sacrificial anode structure and its corrosion evaluation». *Primer Congreso de Corrosión NACE- Región Latinoamericana.* Maracaibo, Venezuela. Pag. 94064/1-94064/12.

[40] Garcia, G., Campillo, B., Genescà, J., Juárez, J., Rodríguez, C., and Martínez, L., (1994), «Influencia de los tratamientos térmicos en un ánodo de magnesio evaluado bajo ASTM G-97-89». *Primer Congreso de Corrosión NACE- Región Latinoamericana.* Maracaibo, Venezuela. Pag. 94056/1-94056/10.

[41] Campillo, B., Rodriguez, C., Juárez, J., Genescà, J. and Martinez, L., (1996), «An Improvement of the Anodic Efficiency of Commercial Mg Anodes». *NACE Corrosion'96*. Houston. Paper # 201. Pag. 201/1-201/18.

[42] Campillo, B., Rodriguez, C., Genescà, J., Juárez-Islas, J., Flores, O. and Martínez, L. (1997) «Effect of Heat Treatment on the Efficiency of Mg Anodes», *Journal of Materials Engineering and Performance* 6, 449-453.

[43] Genescà, J., Rodriguez, C., Juárez, J., Campillo, B. and Martinez, L., (1998), «Assesing and Improving Current Efficiency in Magnesium Base Sacrificial Anodes by Microstructure Control», *Corrosion Reviews* 16 (1-2) 95-125.

[44] Schreiber, C.F. (1986), Sacrificial Anodes in Cathodic Protection: Theory and Practice, V. Ashworth and C.J.L. Booker Editors, Ellis Horwood Ltd., Chichester, England. P. 78-93.

[45] Schrieber, C., (1991[JG11]), in Ashworth, V., Hanawalt, J.D., Nelson, C.E. and Peloubet, J.A., Corrosion Studies of Magnesium Alloys, Metals Technology, September.

[46] Bessone, J.B., Suarez, R.A., De Micheli, S.M., (1981), Sea Water Testing of Al-Zn, Al-Zn-Sn and Al-Zn-In Sacrificial Anodes, Corrosion 37 (9) 533-539.

[47] Tunold, R. (1991), Corrosion Science 17, 533.

[48] Jones, H. (1984), Journal of Materials Science 19, 1043.

[49] Despic, A.R., Drazic, D.M., Purenovic, M.M. and Cikovic, N., (1976), Electrochemical properties of Al Alloys Containing In, Ga and Tl, Journal of Applied Electrochemistry 6, 527.

[50] Salleh, M., (1978), Ph. D Thesis, UMIST, Manchester, U. K.

[51] Clark, J.B., Aronson, H. and Domian, H.A., (1961), Retrograde movement of alpha:beta brass boundaries, Trans. Am. Soc. Met., 53, 295.

[52] Kuznetsov, G.M., Barsukov, A.D., Krivosheeva, G.B. and Dieva, E.G., (1986), A study of phase equilibriums in Al-Zn-Mg alloys, Akad, Nayk, SSSR Met. 4, 198.

[53] Barbucci, A., Cerisola, G., Bruzzone, G. and Saccone, A., (1977), Activation of aluminium anodes by the presence of intermetallic compounds, Electrochimica Acta, 42 (15) 2369.

[54] Kilmer, R.J. and Stonere, G.E., (1991), The effect of Zn addition on the enviromental stability of Al-Li alloys, Light Weight Alloys for Aerospace Applications II, TMS, 3.

[55] Petrov, D.A., (1993), in Ternary AlloysA comprehensive compendium of evaluated comstitutional data and phase diagrams, eds G. Petzow and G. E. Effemberg, VCH Verkgsgesellschaft 7, 57.

[56] Zhand, X.,Wang, Y. and Huo, S (1995), Study on electrochemical properties of Al-Zn-Mg-In-Ca alloy sacrificial anode, Corrosion Science and Protection Technique , 7 (1) 53.

Acknowledgements

The authors would like to thank other staff and students of the Universidad Nacional Autónoma de México, UNAM, who have contributed to our understanding of the subject. We would like to recognize the contributions of our students Juan C. Lee, Luis Betancourt, Liliana Jerade, Marco Talavera, José T. Pérez, Mario Suarez and Socorro Valdez, and colleagues Bernardo Campillo, Lorenzo Martinez, Ramiro Perez and Carlos Rodriguez.

One of the authors, JG, wishes to thank Consejo Nacional de Ciencia y Tecnologia, CONACYT, and Dr. Luis Ximenez Caballero for financial support during sabbatical leave.

This research continues to receive support from DGAPA-UNAM and CONACYT.

About the authors

Joan Genescà i Llongueras born in Terrassa, Catalonia, in 1949. Doctor in Chemical Engineering (1980) from the Institut Quimic de Sarriá, IQS, since 1982 he has been full professor of Electrochemistry and Corrosion Engineering at the Department of Metallurgical Engineering, School of Chemistry, UNAM. Co-author of the series of books «Mas allá de la herrumbre», (Beyond Rust), edited by Fondo de Cultura Económica, México, he has published another book about atmospheric corrosion and one textbook on the thermodynamic and kinetic principles of corrosion. His research is on the various aspects of corrosion and corrosion engineering, specially cathodic protection and electrochemical methods in corrosion research. He is a member of the Societat Catalana de Química (IEC), National Association of Corrosion Engineers (NACE), the Electrochemical Society and the Academia Nacional de Ingeniería (México).

Julio Juárez-Islas received his bachelor degree in Metallurgy from the Department of Metallurgy, Faculty of Chemistry-UNAM in 1980. In 1982, he obtained his Diploma in Metallurgy and, in 1987, his PhD. Degree in Metallurgy, from the School in Materials at Sheffield University. From 1986 to 1999 was invited to collaborate with the Royal Airforce Establishment in the field of rapid solidification of light alloys. Currently, he is working at the National University of Mexico as a full professor in the field of Development of New Materials. His research has been awarded three national prizes and one international prize in the field of Development of Technologies.